Check for updates

ACES Asian Chemical Editorial Society

doi.org/10.1002/cnma.202300566

CHEMNANOMAT
Review

www.chemnanomat.org

Colloidal Plasmonic Metasurfaces for the Enhancement of Non-Linear Optical Processes and Molecular Spectroscopies

Ylli Conti,*[a] Naihao Chiang,[b] and Leonardo Scarabelli*[a]

Colloidal metasurfaces are emerging as promising candidates for the development of functional chemical metamaterials, combining the undisputed control over crystallography and surface chemistry achieved by synthetic nanochemistry with the scalability and versatility of colloidal self-assembly strategies. In light of recent reports of colloidal plasmonic materials displaying high-performing optical cavities, this Minireview discusses the use of this type of metamaterials in the specific context of non-linear optical phenomena and non-linear molecular spectroscopies. Our attention is focused on the opportunities and advantages that colloidal nanoparticles and self-assembled plasmonic metasurfaces can bring to the table compared to more traditional nanofabrication strategies. Specifically, we believe that future work in this direction will express the full potential of non-linear molecular spectroscopies to explore the chemical space, with a deeper understanding of plasmon-molecule dynamics, plasmon-mediated processes, and surface-enhanced chemistry.

1. Introduction

Photonic metamaterials are artificial structures consisting of subwavelength elements that are rationally designed and arranged (periodically or non-periodically) to generate a unique electromagnetic response.[1–3] Ultimately, this freedom in design leads to the possibility of engineering materials presenting exotic macroscopic properties not found in nature. Since the first theoretical predictions by Vaselago, Yablonovitch, and Pendry,[4–6] and the first experimental verifications by Shelby *et al.*,[7] the field of metamaterials has witnessed a steady exponential growth over the last two decades, offering exceptional flexibility for the manipulation of light-matter interactions, as well as new and exciting possibilities for applications in imaging, photonics, telecommunications, and electronics.[8–13] Due to the need for subwavelength unit cells, the fabrication of metamaterials targeting the visible and infrared (IR) portion of the electromagnetic spectrum posed a major technological challenge compare to the first examples operating in the microwaves, as the components must have nanometric dimensions. These restrictions established a tight feedback loop between metamaterial scientific research and nanofabrication techniques such as optical and electron lithography, which were initially developed for semiconductor manufacturing, and enabled the preparation of metallic plasmonic nanostructures of different geometries and 3-dimensional organization with nanometer-scale precision. Ultimately, these technological and scientific advancements made concepts such as metaoptics and meta-lenses a reality, encompassing architectures capable of manipulating light polarization, phase, and wavefront, as well as controlling both absorption and emission phenomena.[14–17] The possibility of applying engineered artificial optical properties to manipulate light-matter interactions created a fertile area for the exploration of non-linear (NL) phenomena, exploiting the incredible flexibility in the near-field electromagnetic response.

Very recently, the scientific interest around metamaterials led to a new development phase, the so-called "chemistry of metamaterials", where the engineered artificial properties are dynamically modified or enable the dynamic interaction with the surrounding chemical environment. This includes chemically responsive, catalytic, or phase-changing materials as well as the molecular functionalization of the unit cells, enabling receptor-, pH- or electrochemistry-based responses.[18–21] In this scenario, NL optical phenomena offer a unique development opportunity. In fact, molecular spectroscopies based on second- or third-order susceptibilities encode rich molecular information that can be extrapolated directly from their optical response to sense the surrounding chemical space.[22] The successful fabrication of metamaterials for the exploration/interaction with the chemical surroundings imposes new scientific as well as technological challenges. Since they were originally designed for microelectronics development, standard nanofabrication processes (including metal evaporation and hard lithography techniques) offer limited control over the crystallography and surface chemistry of the prepared nanostructures, and reduce, at the same time, the choice of substrate and operating conditions. As such, the pursuit of chemically active metasurfaces led the scientific community to seek alternative fabrication strategies. In this scenario, colloidal self-assembly emerged as promising contender: on one side, colloidal synthesis offers an

[a] Y. Conti, Dr. L. Scarabelli
Institute of Materials Science of Barcelona, ICMAB-CSIC, Campus UAB, Bellaterra 08193, Spain
E-mail: yconti@icmab.es
lscarabelli@icmab.es

[b] Prof. N. Chiang
Department of Chemistry, University of Houston, Houston, Texas 77204, United States
E-mail: nchiang@Central.UH.EDU

© 2024 The Authors. ChemNanoMat published by Wiley-VCH GmbH. This is an open access article under the terms of the Creative Commons Attribution Non-Commercial NoDerivs License, which permits use and distribution in any medium, provided the original work is properly cited, the use is non-commercial and no modifications or adaptations are made.

© 2024 The Authors. ChemNanoMat published by Wiley-VCH GmbH

unmatched level of control over nanoparticle morphology, crystallography, composition, and surface chemistry; on the other side, self-assembly strategies are now capable of producing high-quality periodic and hierarchical arrangements at large scales.

This Minireview presents the most recent progresses made in the use of colloidal-based plasmonic metasurfaces in the context of NL optical phenomena. We first introduced the fundamental theoretical aspects, focusing our attention on the roles played by plasmonic metasurfaces in promoting and controlling NL optical processes and their potential impacts on molecular spectroscopies. In the following section, we reviewed the colloidal self-assembly preparation of these type of systems and provided selective examples from the literature where they were applied for the promotion of NL optical processes. We conclude this review with our perspective on the field's future development. Our aim is to highlight the opportunities offered by colloidal systems as dynamic chemical metastructures towards advanced and versatile NL optical devices.

2. Fundamentals of Non-Linear Optics

When an intense coherent light source interacts with a material, the collective displacement of the charges generating the resulting outgoing electromagnetic fields becomes gradually and asymmetrically distorted, affecting the overall optical response of the system.[23] The intensity of the scattered light will then increase non-linearly with the intensity of the impinging optical field, typically following a square or a cube dependency.[22] Mathematically, the electromagnetic response of a medium at optical frequencies can be described by the polarization vector **P**, which is the result of the combined linear ($\mathbf{P}^{l}$) and non-linear ($\mathbf{P}^{nl}$) polarization vector components and no longer depends linearly on the strength of the applied electric field **E**. Assuming an input field polarization along the $\bar{x}$ direction, the expression can be expanded in power series as:[22]

$$\mathbf{P}_i = \varepsilon_0 \left[\chi_{ij}^{(1)} \mathbf{E}_j + \chi_{ijk}^{(2)} \mathbf{E}_j \mathbf{E}_k + \chi_{jkl}^{(3)} \mathbf{E}_j \mathbf{E}_k \mathbf{E}_l + \ldots \right] = \mathbf{P}_i^{l} + \mathbf{P}_i^{nl} \quad (1)$$

$$\mathbf{P}_i^{nl} = \varepsilon_0 \left[\chi_{ijk}^{(2)} \mathbf{E}_j \mathbf{E}_k + \chi_{jkl}^{(3)} \mathbf{E}_j \mathbf{E}_k \mathbf{E}_l + \ldots \right] = \mathbf{P}_i^{(2)} + \mathbf{P}_i^{(3)} + \quad (2)$$

where ε_0 is the vacuum permittivity, $\chi^{(1)}$ is the linear susceptibility of the medium, describing light-matter interaction processes such as absorption and emission, and $\chi^{(2)}$ and $\chi^{(3)}$ are, respectively, the second- and third-order NL susceptibility describing higher orders NL phenomena (in this notation the order of the tensor is represented by the upper index (1), (2), (3); the lower index *ijk* denote the vector component implicitly summed). By substituting an incident monochromatic electromagnetic field $\mathbf{E}(\mathbf{r},t) = \mathrm{E}_0 e^{i(\mathbf{k}\cdot\mathbf{r}-\omega t)}$ impinging on the material into Eq. 1, the NL terms of the polarization ($\mathbf{P}_i^{(2)}$ and $\mathbf{P}_i^{(3)}$) can oscillate at different frequencies without violating the conservation of energy, giving rise to phenomena such as second (2ω) and third (3ω) harmonic generation (respectively SHG and THG, Fig-

Ylli Conti completed her studies in Science and Engineering of the Innovative and Functional Materials at the University of Calabria (Italy), with a master's thesis work based on the characterization of plasmonic metasurfaces applied in SERS analysis of HAV virus. She is currently working as Ph.D. student at the Institute of Materials Science of Barcelona (ICMAB), under the supervision of Dr. Leonardo Scarabelli. Her research focuses on the use of plasmonic metasurfaces fabricated via alternative methods (soft-lithography and self-assembly) that operate in the weak and strong coupling regime, to study the influence of light-matter interactions on the landscape of chemical reactions.

Naihao Chiang received his bachelor's degrees in physics, chemistry, and economics/mathematics from the University of Southern California. In 2017, he received his Ph.D. from Northwestern University under the supervision of Profs. R. P. Van Duyne and T. Seideman. Since 2021, he has been appointed as the Drs. Yao and Song Endowed Assistant Professor of Chemistry at the University of Houston. Dr. Chiang's research group focuses on developing near-field spectroscopy and microscopy in the liquid phase and investigating fundamental chemical processes under intense optical fields.

Leonardo Scarabelli completed his studies in chemistry at the University of Pavia, and in 2016 he received his Ph.D. from the University of Vigo under the direction of Prof. L. M. Liz-Marzán. After training as a postdoctoral scholar at UCLA, he began his independent career at the Institute of Materials Science of Barcelona (ICMAB) as a "La Caixa" Junior Leader. In 2023, he was awarded an ERC Starting Grant with his project NANOGROWDIRECT. His scientific interests include the development of unconventional strategies for the direct surface synthesis of plasmonic arrays, and their implementation into weakly and strongly coupled materials.

© 2024 The Authors. ChemNanoMat published by Wiley-VCH GmbH

2199692x, 2024, 4, Downloaded from https://aces.onlinelibrary.wiley.com/doi/10.1002/cnma.202300566 by Universidad De Cantabria, Wiley Online Library on [07/08/2024]. See the Terms and Conditions (https://onlinelibrary.wiley.com/terms-and-conditions) on Wiley Online Library for rules of use; OA articles are governed by the applicable Creative Commons License

ure 1a). Similarly, when the incident field is formed by a superposition of two plane waves:

$$\mathbf{E}(\mathbf{r},t) = \mathbf{E}_1\, e^{i(k1\cdot r-\omega 1t)} + \mathbf{E}_2\, e^{i(k2\cdot r-\omega 2t)} + cc \quad (3)$$

where k_1 and k_2 are the wave vectors, ω_1 and ω_2 are the corresponding frequencies of the two interacting tones, and *cc* is the complex conjugation, the NL terms can oscillate at frequencies $\omega_1 \pm \omega_2$ giving rise to sum (SFG) and difference (DFG) frequency generation (Figure 1a).[22] These frequency conversion processes probe the second-order susceptibility $\chi^{(2)}$, and gained significant attraction in the last decade, finding applications in photonics, holography, and invisible cloaking technology. In parallel, NL spectroscopies were developed to extrapolate chemical information from $\chi^{(2)}$ and even the third-order susceptibility $\chi^{(3)}$, bringing new solutions for biosensing, imaging, and studies of ultrafast dynamics. Similarly to first-order light-matter interactions, high-order phenomena are also subjected to symmetry rules constraints originated from material's electronic structure. In centrosymmetric structures, characterized by an inversion symmetry center, the structural properties remain unchanged upon any symmetry transformation. That is, considering an imaginary line passing through the center of the structure, for each point with coordinates (x, y, z), after an inversion operation, the corresponding point (−x, −y, −z) describes the same structure. Here, when an opposite electric field (−**E**) is applied, the second-order polarization results in $-\mathbf{P}_i^{(2)} = \mathbf{P}_i^{(2)}$, implying that $\chi^{(2)}$ must be zero (a similar argument is valid for $\chi^{(3)}$ and higher orders). Ultimately, this observation leads to the conclusion that the properties for centrosymmetric structures remain unchanged under an external influence and do not show any NL responses. A symmetry breaking is therefore necessary to perturbate the system, leading to the emergence of NL effects. Frequency conversion processes can originate from the surface's asymmetries associated with small deviation from perfect symmetrical shape,[24,25] and most metals show second-order effects originating from NL dipoles at metal surfaces, where symmetry breaking occurs.[26] Finally, multipolar plasmonic resonances, arising from retardation effects associated with nanoparticle size and morphology, can induce a NL optical response.[25,27–29]

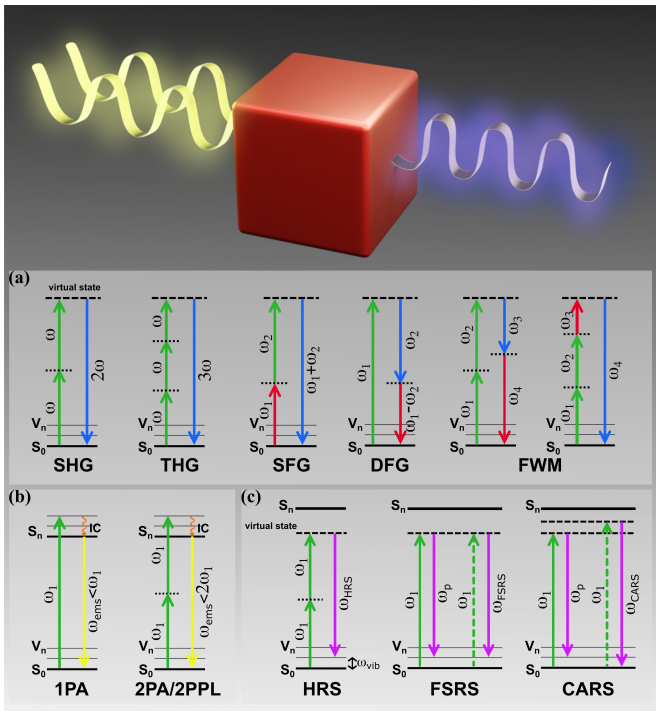

Figure 1. Jablonski diagrams of the most common non-linear optical processes. (a) From left to right: second harmonic generation *(SHG)*, third harmonic generation *(THG)*, sum frequency generation *(SFG)*, difference frequency generation *(DFG)*, and four-wave mixing *(FWM*, non-degenerate case*)*. The dashed lines represent the virtual excited energy states, while the solid grey lines represent the vibrational energy levels. S_0 represents the ground singlet (electronic) energy state, S_n is the n-th singlet (electronic) excited level, and V_n represents the n-th vibrational energy level of the singlet ground energy state (S_0). **(b)** From left to right: comparison between the one- and two-photon absorption processes, respectively one-photon absorption *(1PA)* and two-photon absorption *(2PA)*. These two processes involve the emission of a photon after the internal conversion (*IC*) of the excited electron to the lowest vibrational state of S_n (Kasha's rule). **(c)** Vibrational spectroscopies processes exploiting different photon energies and interactions. These processes involve the inelastic scattering of photons, resulting in a shift in the frequency of the scattered light. Since they are non-degenerate processes, the frequency of the scattered light is different from the incident light. From left to right: hyper Raman scattering *(HRS)*, femtosecond stimulated Raman scattering *(FSRS)*, and coherent anti-Stokes Raman scattering *(CARS)*. ω_p is the probe frequency, and ω_{vib} is the vibrational frequency.

All the NL optical processes mentioned so far are known as *parametric* processes, in which the system has identical initial and final quantum-mechanical states. Here, the conservation of energy and momentum of the interacting photons is achieved through the NL medium, enabling the ground-level population to transit through virtual energetic levels.[22] Instead, processes involving the transfer of population from one real quantum-mechanical state to another are known as *non-parametric* processes, and the energy of the interacting electromagnetic radiation can be transferred to or from the medium.[22] Examples of non-parametric NL processes include two-photon absorption (2PA), two-photon excited photoluminescence (2PPL), and almost all NL optical spectroscopic processes, as schematized in Figure 1b and c. In all cases, the transition from the ground state to an excited state occurs through the simultaneous absorption of two photons with sufficientenergy to promote an electron from one level to the other. These phenomena had a significant impact on the development of two-photon microscopy, allowing deeper tissue penetration with less photodamage compared to traditional single-photon bio-imaging techniques.

3. Plasmonics Metasurfaces and Non-Linear Light-Matter Interactions

One major driving force behind the development of plasmonic metasurfaces is their capability to increase the efficiency of light-matter interactions by orders of magnitudes at specific frequencies, taking advantage of the strong confinement and near-field enhancement of the electromagnetic fields in the

© 2024 The Authors. ChemNanoMat published by Wiley-VCH GmbH

2199692x, 2024, 4, Downloaded from https://aces.onlinelibrary.wiley.com/doi/10.1002/cnma.202300566 by Universidad De Cantabria, Wiley Online Library on [07/08/2024]. See the Terms and Conditions (https://onlinelibrary.wiley.com/terms-and-conditions) on Wiley Online Library for rules of use; OA articles are governed by the applicable Creative Commons License

proximity of metallic nanostructures.[23,30] The first example of plasmonic-enhanced spectroscopy can be traced back to the 1970s and 1980s with the discovery of surface-enhanced Raman spectroscopy (SERS),[31,32] where $>10^5\times$ enhancement of the Raman signal intensity was predominantly attributed to the the local electric field amplification (the so-called electromagnetic mechanism).[33] Since these first experimental demonstrations, the rational design of plasmonic nanostructures made a huge step forwards, going from simple disordered colloids,[34] to complex multi-resonant and combined nanostructured arrays (with active and passive elements).[35]

3.1. Plasmonic Metasurfaces and Non-Linear Optics

Currently, metasurfaces can display a virtually unlimited variety of shapes and compositions (Figure 2), including nanoholes,[36–38] nanoparticles,[39–41] pillars,[42,43] chiral shapes,[44–48] and antennas,[49–52] translating directly into an incredible versatility of their optical response, which can be tuned by modifying both the localized plasmonic response of each repeating unit, as well as the geometrical parameters of the array. These parameters will ultimately regulate the quality and the spectral position of all localized and collective resonances, driving the boost of quantum efficiency of the various NL optical processes.[53–55] Moreover, these properties also convey the exceptional ability of shaping the wavefront of light with subwavelength resolution.[56] This ability is essential to overcome the phase matching condition requirements ($\Delta k = k_{out} - nk_{in} = 0$ where k_{out} is the wavevector of the converted frequency and k_{in} are the wavevectors of the input frequencies, and n is an integer),[57–59] as the additional momentum provided by the structure with periodicity Λ ($\Delta k\ (\Lambda) = k_{out} - nk_{in} - G(\Lambda) = 0$, where $G(\Lambda)$ is the wavevector associated to the grating), guarantees that the momentum is conserved, allowing an efficient NL conversion over extended interaction length.

Exploiting this versatility, Czaplicki *et al.* explored the inclusion of passive elements (centrosymmetric dielectric nanobars) in a plasmonic metasurface constituted of non-centrosymmetric L-shaped metallic units. The modification of the near-field distribution, mediated by the coupling through lattice interactions, led to an improvement of the SHG enhancement.[35] A further increment of an order of magnitude was achieved in a later study by improving the spectral match between the surface lattice resonance of the array and the frequency of the impinging electromagnetic radiation.[53] Another exciting possibility is to use an anisotropic plasmonic bandgap to control the directionality of the NL optical response. This effect was explored by Kolkowski R. and coworkers through the fabrication of a 2D rectangular array of non-centrosymmetric metallic pyramids by depositing a 100 nm silver layer on top of a patterned GaAs substrate. The obtained anisotropic band gap not only gave rise to a substantial field enhancement through the excitation of band edge modes at the fundamental frequency, but the presence of surface plasmon polaritons (SPP) contributed to break the symmetry of the system and achieve

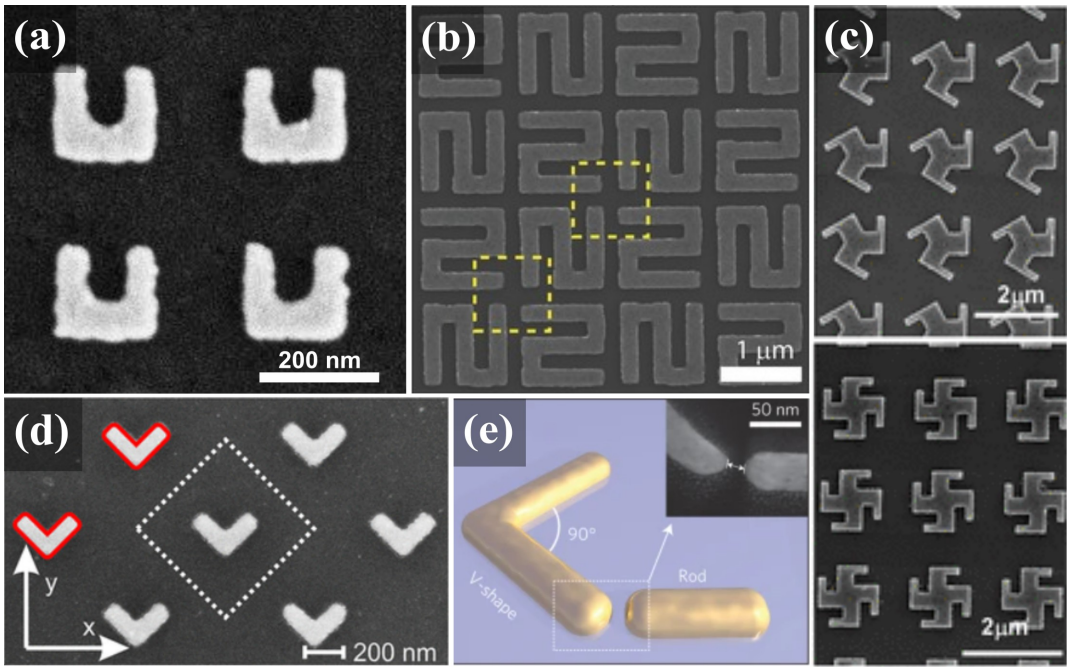

Figure 2. Plasmonic metasurfaces for strong non-linear optical responses. Scanning Electron Microscopy (*SEM*) images of **(a)** gold split-ring resonator square arrays; **(b)** *Rodovik* traditional Slavic symbol, consisting in identical (not mirrored) interspaced unit cells, showing non-linear chiroptical response by optimization of gap size and design; **(c)** *Trisceli-* (**above**) and *Gammadion*-type (**below**) geometry for second and third non-linear response respectively, displaying near-unity circular dichroism; breaks of symmetry achieved by using plasmonic structures such as **(d)** non-centrosymmetric V-shaped gold nanoparticles, and **(e)** multiresonant antennas for *SHG* response. **Panel a**: Copyright 2012, APS. Adapted with permission.[64] **Panel b:** Copyright 2014, Wiley-VCH. Adapted with permission.[65] **Panel c**: Copyright 2020, ACS. Adapted with permission.[45] **Panel d**: Copyright 2018, ACS. Adapted with permission.[66] **Panel e**: Copyright 2020, Springer Nature. Adapted with permission.[67]

© 2024 The Authors. ChemNanoMat published by Wiley-VCH GmbH

2199692x, 2024, 4, Downloaded from https://acces.onlinelibrary.wiley.com/doi/10.1002/cnma.202300566 by Universidad De Cantabria, Wiley Online Library on [07/08/2024]. See the Terms and Conditions (https://onlinelibrary.wiley.com/terms-and-conditions) on Wiley Online Library for rules of use; OA articles are governed by the applicable Creative Commons License

complete control over SHG anisotropy.[60] The anisotropic control driven by the SPP allows the directional emission of a second harmonic response. The ability to control SHG anisotropy is crucial, for example, in the development of optical switches and modulators offering potential applications in telecommunications and quantum information processing.More complicated geometries, including Fano-type resonances[61] and waveguided-assisted split-ring resonator array, were also explored.[62] The role of plasmonic metasurfaces is not only restricted to the enhancement of NL signal intensity. For example, Almeida and coworkers applied similar architectures to encode phase information for the reconstruction of images (phase holograms).[63] Specifically, they exploited the concept of NL phase control to reconstruct THG holograms, where the image is formed at a wavelength different from the reading beam. The authors used V-shaped nanoantennas, with specific polarization dependency, without plasmonic resonance matching the third harmonic frequency. Since the phase didn't change during the propagation of the fundamental electromagnetic wave through the sample, they were able to build up a multilayer structure. A distinct phase hologram was computer-generated for each layer within the metamaterial, yielding to reconstruct the far-field image by using specific polarized input beam (vertically and horizontally). This approach offered higher data density compared to flat metamaterials, due to the individual element dimension being much smaller than the optical wavelength, enabling it to overcome the optical diffraction limitation.

3.2. Towards Non-Linear Molecular Spectroscopies Enabled by Plasmonic Metasurfaces

Plasmonic metasurfaces near-field enhancement was also applied to the development of NL molecular spectroscopies. Here, understanding the spatial distribution and spectral response of the near-field becomes even more significant, as the molecular surface distribution will directly impact their contribution to the overall signal. For example, the higher enhancing nature of coupled plasmons leads to the creation of regions of high electric-field confinement, contributing to most of the detected signal, generally referred to as "hot spots". These highly enhancing regions were mapped using high-resolution molecule-substrate distance dependence SERS,[68] as well as super-resolution fluorescence microscopy,[69] electron energy loss spectroscopy and cathodoluminescence,[70–72] and scanning probe microscopy.[73] On the other hand, the spectral dependency of the near-field was studied in detail *via* wavelength-scanned surface-enhanced Raman excitation spectroscopy (WS-SERES),[74] demonstrating how the relative spectral position of the localized surface plasmon resonance and the molecular electronic transition can modify the right choice of excitation wavelength for maximizing the enhancement of the Raman signal.[75]

Extending these analyses to NL spectroscopies to fully understand the spatial and spectral influence on the chemical systems by multiple plasmonic resonance modes, would be extremely valuable. Nonetheless, the general concepts underlying these effects can be extrapolated to plasmonic near-field enhanced or surface-enhanced NL optical spectroscopy (SE-NLOS). In this molecular context, the power series expansion of polarization presented in equation (**1**) can be rewritten as:

$$\mathbf{P}^{(1)} = \alpha\mathbf{E}, \quad \mathbf{P}^{(2)} = \frac{1}{2}\beta : \mathbf{EE}, \quad \mathbf{P}^{(3)} = \frac{1}{6}\gamma : \mathbf{EEE} \tag{4}$$

Where α, β, and γ represent the molecular polarizability, 1st hyperpolarizability, and 2nd hyperpolarizability tensors, respectively. Consequently, optical spectroscopies can exhibit different dependence on the strength of the plasmonically enhanced optical fields, and SE-NLOSs can achieve even higher enhancement factors, ultimately allowing the detection and analysis of molecular and interfacial events that would be challenging or impossible to observe using non-enhanced NL optical techniques. In fact, while SERS intensity (I) scales as $\sim|\mathbf{E}|^4$, for 2nd order processes with two incoming laser fields and one outgoing radiation $I \propto |\mathbf{E}_{out}|^2|\mathbf{E}_{in1}|^2|\mathbf{E}_{in2}|^2 \sim |\mathbf{E}|^6$, assuming that the plasmonic resonance frequencies match all three optical fields. Similarly, the 3rd order processes can present enhancements up to $\sim|\mathbf{E}|^8$.[76]

As an extension of SERS,[77,78] surface-enhanced hyper Raman spectroscopy (SE-HRS) was one of the earliest demonstrations of second-order SE-NLOS. The Jablonski diagram suggests that the enhancement of the HRS signal requires a resonance overlapping with both the pump frequency ω_1 or/and ω_{HRS} ($\omega_{HRS} = 2\omega_1 - \omega_{vib}$, Figure 1c).[79] Using non-colloidal plasmonic metasurfaces, SE-HRS has been used to probe symmetry at the electrode/solution interface (Figure 3a).[80] In this work, complementary HRS vibrational normal modes were used in addition to SERS to understand the specific absorption site of pyridines on a silver plasmonic electrode while following the electrochemical reaction, highlighting the extra chemical information SE-HRS can generate.

Another powerful second-order SE-NLOS is surface-enhanced vibrational sum frequency generation spectroscopy (SE-vSFG). Since β is a function of the tensor product of polarizability and IR transition dipole moment, vSFG has non-zero signals for vibrational transitions that are both Raman and IR active. At the same time, isotropic bulk medium and centrosymmetric molecules do not exhibit a vSFG signal, as the overall $\chi^{(2)}$ is zero. This unique property of vSFG makes it particularly suitable for studying interfaces where the symmetry is broken. While the vSFG signal from setups with pulsed lasers and modern detectors is sufficient for many self-assembled molecular systems, plasmonic enhancement may still be desirable for studying systems with a low number of molecules or molecules characterized by a small hyperpolarizability. For example, Baldelli *et al.* used Pt nanoparticle arrays with a plasmon resonance in the IR for studying CO absorption with $\sim 10^4$ enhancement.[81] This study revealed the potential of tracking a catalytical reaction that would otherwise be impossible without the plasmonic enhancement (Figure 3b).

Despite their incredible potential, second order SE-NLOS on plasmonic metasurfaces did not witness the same exponential

© 2024 The Authors. ChemNanoMat published by Wiley-VCH GmbH

2199692x, 2024, 4, Downloaded from https://aces.onlinelibrary.wiley.com/doi/10.1002/cnma.202300566 by Universidad De Cantabria, Wiley Online Library on [07/08/2024]. See the Terms and Conditions (https://onlinelibrary.wiley.com/terms-and-conditions) on Wiley Online Library for rules of use; OA articles are governed by the applicable Creative Commons License

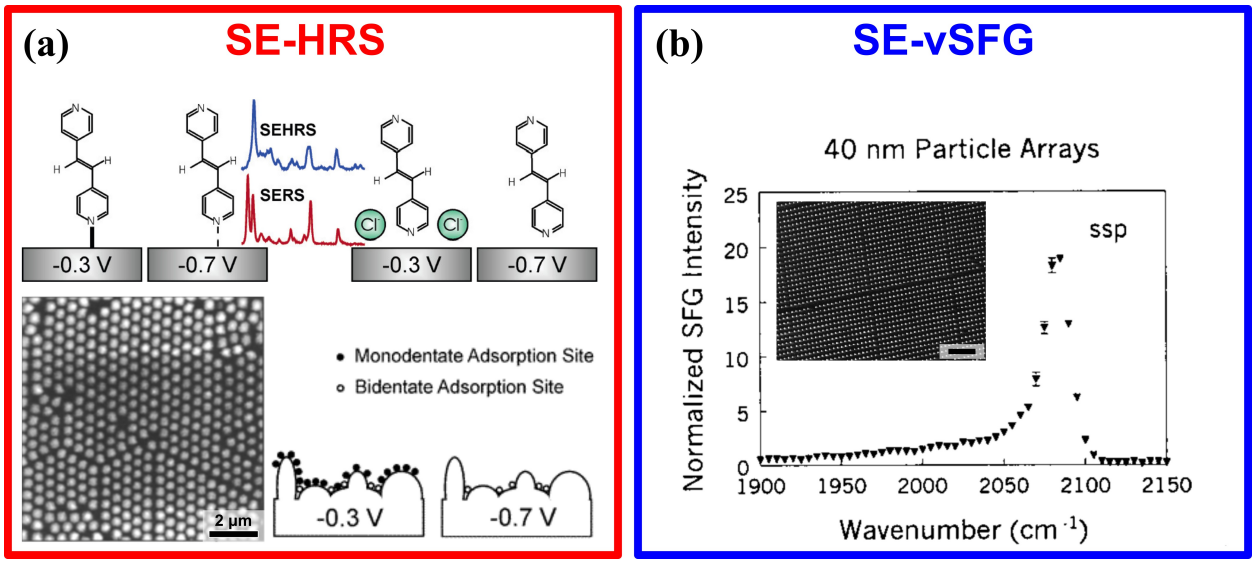

Figure 3. Plasmonic metasurfaces for non-linear molecular spectroscopies. **(a)** Electrochemical surface-enhanced hyper Raman scattering of centrosymmetric molecules on silver film over polystyrene nanospheres electrodes. The monodentate site refers to the surface binding via a single nitrogen of the molecule trans-1,2-bis(4-pyridyl)ethylene, reducing the site symmetry, and inducing the appearance of the *SE-HRS* band. On the other hand, the bidentate bridging site refers to the surface binding of the same molecule via both nitrogen atoms, maintaining symmetry and not contributing to the *SE-HRS* band. **(b)** Surface-enhanced vibrational sum frequency generation spectra of CO adsorbed on 40 nm platinum nanoparticle arrays (**Inset** scale bar 1 μm). **Panel a**: Copyright 2006, ACS. Adapted with permission[80] and Copyright 2002, ACS. Adapted with permission.[82] **Panel b**: Copyright 2000, ACS. Adapted with permission.[81]

growth observed for SERS. In fact, even with signal enhancement several orders of magnitude bigger, SE-NLOSs remain a significant challenge since the magnitude of the hyperpolarizabilities decreases as much as ~10^{-10} when the order of the associated NL optical processes increases. Finding a robust fabrication method for plasmonic substrates that can enhance all optical fields involved in the process would be pivotal to developing SE-NLOS.

4. Colloidal Self-Assembly for Plasmonic Metasurfaces

As evidenced by the highlighted examples, the experimental investigation of NL optical phenomena relied on developing advanced nanofabrication techniques to prepare high-quality plasmonic metasurfaces. By improving the confinement of the associated electromagnetic field, these technological progress ultimately boosted the optical non-linearity in materials response at low pump intensities, avoiding the need for complex phase matching techniques.[83,84] Most of these fabrication processes fall within the realm of hard lithography, including extreme ultraviolet (UV) lithography, focused ion-beam (FIB), electron beam lithography (EBL) and thermal evaporation steps. However, fabrication methodologies relying on soft-lithography such as nanoimprint lithography,[85] micro-contact printing,[86–88] colloidal self-assembly,[89–95] and *in situ* growth[96,97] are emerging as promising alternatives capable of bringing plasmonic metamaterials to the next development phase. On one side, constant progress in the field of colloidal chemistry has enabled great advances in the synthesis of plasmonic nanoparticles, leading to unprecedented control of optical properties by controlling elemental composition, near-field distribution, and even chirality at the single nanoparticle level.[98–100] At the same time, developments in surface chemistry, feature miniaturization, and scalability had a huge impact on the quality of the fabricated colloidal-based metasurfaces, controlling the distribution and orientation of single nano-objects, targeting high-quality factor plasmonic optical cavities and achieving high-throughput large-scale self-assembly up to wafer-scale dimensions.

Examples of colloidal self-assembly approaches include drop casting,[101] spin coating,[102,103] and Langmuir-Schaefer techniques.[104,105] Still, the two strategies that achieved the most widespread results are perhaps capillary-assisted particle assembly (CAPA) (Figure 4a) and template-assisted self-assembly (TASA) (Figure 4b), where nanoparticle concentration is induced in accumulation zones of the liquid meniscus *via* convective flow. Controlling the evaporation rate, the features of the template define a minimum in free energy that selectively traps the nanoparticles.[106–108] CAPA is particularly successful in forming single-particle metasurfaces, *i.e.*, where the repeating unit is a single plasmonic nanoparticle. This approach recently yielded quality factors above 50,[109] and it was expanded to the organization of anisotropic nanoparticles such as cubes or rods.[109–111] The main drawback of this approach is that the nanoparticles assemble inside nanocavities previously prepared on the substrate, and the fabrication process must involve either a transfer printing step,[109,110,112,113] or a dissolution step.[114] On the other side, TASA has greatly improved reproducibility and precise control of the spatial organization of

© 2024 The Authors. ChemNanoMat published by Wiley-VCH GmbH

2199692x, 2024, 4, Downloaded from https://acses.onlinelibrary.wiley.com/doi/10.1002/cnma.202300566 by Universidad De Cantabria, Wiley Online Library on [07/08/2024]. See the Terms and Conditions (https://onlinelibrary.wiley.com/terms-and-conditions) on Wiley Online Library for rules of use; OA articles are governed by the applicable Creative Commons License

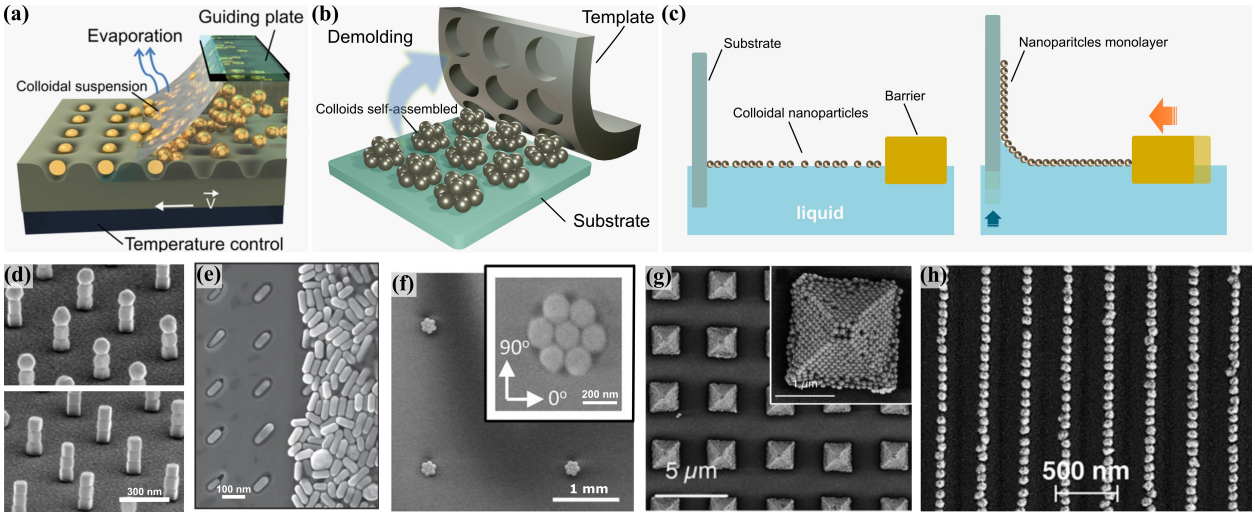

Figure 4. Colloidal-based plasmonic metasurfaces fabricated *via* soft-lithographic strategies. Scheme of **(a)** capillary-assisted particle assembly (*CAPA*), **(b)** template-assisted self-assembly (*TASA*), and **(c)** Langmuir-Blodgett deposition fabrication methods. *SEM* images of: **(d)** Template-DNA-mediated assembly of gold nanoparticles; **(e)** *CAPA* of gold nanorods; *TASA* of **(f)** heptamers nanoclusters, and **(g)** pyramidal super-crystals; **(h)** nanoparticles assembled by spin coating on top of a wrinkled polydimethylsiloxane substrate and then transferred onto flat substrates by wet contact printing. **Panel a**: Copyright 2020, Wiley-VCH. Adapted with permission.[89] **Panel d**: Copyright 2018, Science. Adapted with permission.[123] **Panel e**: Copyright 2017, Springer Nature. Adapted with permission.[110] **Panel f**: Copyright 2012, ACS. Adapted with permission.[124] **Panel g**: Copyright 2017, ACS. Adapted with permission.[125] **Panel h**: Copyright 2014, ACS. Adapted with permission.[112]

the colloidal meta-units. Indeed, the templates are often designed to engineer specific interactions with nanoparticles based on size, shape, and chemistry,[92] ensuring quality factors >60 and enough efficiency to promote NL phenomena such as lasing emission.[115] This feature offers the possibility of engineering three different plasmonic responses within the same metasurfaces (*i.e.*, the single colloidal response, the localized response of the repeating unit, and the collective response of the lattice), opening fascinating possibilities for the promotion of SE-NLOS. Another significant advantage of TASA is the possibility of performing the assembly directly on the substrate of choice without needing a mask or any other alignment tool. Mayer and coworkers, for example, used this technique to build up a functional magnetic metasurface with high sensitivity, which translated in a sharp drop of the magnetic response, due to a strong coupling between a gold film with one dimension gold nanorods lines assembled on top, targeting advanced sensing applications.[116]

Recently, several template-free alternatives to CAPA and TASA gained much attention in the metamaterial community. A prime example is certainly the packing of plasmonic nanoparticles at the liquid-liquid or liquid-air interface exploiting specifically designed coatings or polymer shells. The obtained self-organized metasurfaces are then transferred to a solid substrate *via* dip-coating or evaporating the liquid phase. Volk *et al.* demonstrated the fabrication of cm^2-scale hexagonally ordered arrays of silver@gold-poly-*N*-isopropylacrylamide core-shell nanoparticles to achieve narrow spectral features.[117] The main drawback of this approach is that it relies on packed colloidal self-assembly, which limits the technique to hexagonal close-packed structures. A step forward in overcoming this limitation was presented by Fernández-Rodríguez *et al.* in 2018, with a variety of tunable particle arrays being prepared by sequential self-assembly and deposition of two differently sized microgel particles at liquid-liquid interfaces (Figure 4c). With a two-step process, they were able to transfer the microgel nanoparticles onto silicon substrates realizing complex non-close-packed binary nanopattern in order to achieve a 2D binary colloidal alloys kinetically inaccessible by direct co-assembly.[118]

Finally, it is worth mentioning recent progress in the development of patterned *in situ* growth directed by chemical contrast.[97,119–121] Despite being still in its infancy, this approach would avoid the need for pre-synthesis, ligand exchange, and self-assembly steps, offering a new toolbox for developing dynamic and chemically active metamaterials. As a first demonstration of this potential, surface lattice resonances were recently recorded as the result of a 100% *in situ* growth process.[122]

5. Non-Linear Optical Properties in Colloidal Systems

Before moving on to the application of colloidal metasurfaces for NL optics, it is important to highlight that isolated noble-metal nanoparticles can exhibit optical non-linearities such as SHG and 2PA.[126–131] The enhancement of the quantum yield of gold photoluminescence following the excitation of localized surface plasmon resonances was first demonstrated by Boyd *et al.* in 1983.[132] In the particular case of gold, two-photon luminescence is a two-step process:[133] the first photon excites one electron from the *sp*-band to an unoccupied energy level above the Fermi level, while the second photon promotes one electron from the lower *d*-band to the unoccupied *sp*-

© 2024 The Authors. ChemNanoMat published by Wiley-VCH GmbH

2199692x, 2024, 4, Downloaded from https://acses.onlinelibrary.wiley.com/doi/10.1002/cnma.202300566 by Universidad De Cantabria, Wiley Online Library on [07/08/2024]. See the Terms and Conditions (https://onlinelibrary.wiley.com/terms-and-conditions) on Wiley Online Library for rules of use; OA articles are governed by the applicable Creative Commons License

conduction band. The two electrons subsequently move closer to the Fermi level *via* intraband relaxation, from which electron-hole recombination can occur through a photon emission process.[134–136] The photoluminescence properties of metal nanoparticles[137] and clusters[138] were exploited for multiphoton microscopy,[139] allowing deeper imaging of biological systems while reducing at the same time the radiation-damage caused to cells and tissues.[140] Recently, Wang and El-Khoury used a near-field scanning probe microscope to image the spatial distribution of SHG, SFG, 2PPL and FWM of a silver nanocube coupled to a gold-coated atomic force microscopy tip.[141] This work elucidated the NL optical properties of a single nanocube when coupled to another plasmonic resonance (Figure 5). However, when compared to organic molecules and semiconductors, the photoluminescence efficiency in metal nanoparticles is significantly weaker, and the emitted light generally presents broader spectral features.[142] The lower performances are caused by non-radiative energy processes of the photo-excited carriers in the metals, such as Coulomb carrier-carrier scattering and electron-phonon interactions, which take place on a faster timescale compared to the electronic relaxations needed for the emission process to occur. This results in a heating effect and a consequent quenching of photoluminescence.[143]

5.1. Colloidal Metasurfaces for Non-Linear Optics

As we explained in section 3, better NL performances can be obtained through the combination of plasmonic metasurfaces with semiconductors or molecular emitters exploiting the electric field enhancement in the proximity of the metal surfaces. Moreover, collective resonances commonly associated with this type of structure are able to overcome the optical losses associated with localized plasmons.[144]

Liu and coworkers, for example, used colloidal silver cubes over a gold mirror to enhance the two-photon photochromism of the spiropyrans/merocyanine system.[145] The large Purcell enhancement in the gap region of the film-coupled nanoparticles led to high directionality and efficiency of the spontaneous emission rate and quantum yield of merocyanine.

In 2023, Conti *et al.* reported lasing of a one-photon excited gain medium stimulated by silver colloidal plasmonic metasurfaces fabricated *via* TASA (Figure 6a–c), achieving on- and off-normal emission with thresholds as low as 0.3 mJ/mm^2.[115] The reported system holds interesting characteristics in the direction of chemically active metamaterials, featuring an optical cavity that remains exposed to the surrounding environment, as the silver nanoparticle arrays were fabricated on top of a waveguiding material layer hosting the gain medium. In this way, they were able to support the outcoupling of plasmonic lattice resonances without using index matching layers, leaving at the same time the cavity accessible for further chemical functionalization.

In another example, Zeng *et al.* demonstrated how colloidal-based metasurfaces are promising structures for the promotion of NL frequency conversion processes such as SHG and upconversion (Figure 6d).[146] They have used silver nanocubes-on-metal geometry, fabricated *via* Langmuir-Blodgett deposition, to create a metamaterial absorbing NIR light and emitting a second harmonic in the visible part of the electromagnetic spectrum. It was determined that both the near-field and plasmonic modes coupling are critical parameters for the enhancing mechanism of SHG. However, the poor spatial phase matching of the SHG far-field signal makes it incoherent. This aspect can potentially be improved by engineering the geometry of the colloidal metasurface.[146]

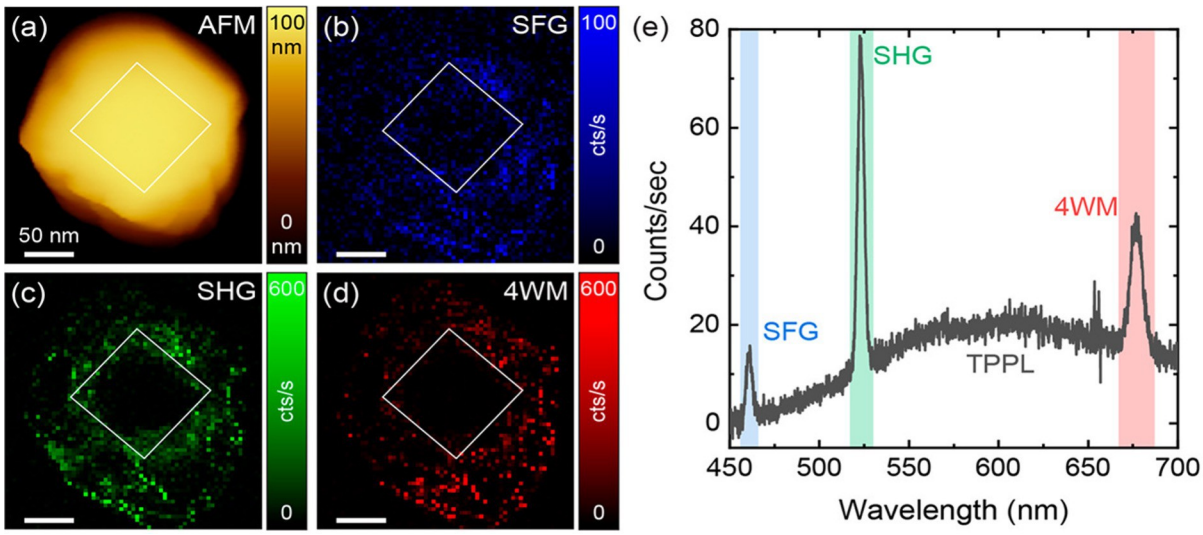

Figure 5. Single nanoparticle non-linear optical response. Silver nanocube (100 nm) **(a)** atomic force microscopy and near-field **(b)** *SFG*, **(c)** *SHG*, and **(d)** *FWM* (or *4WM*) images, spectrally integrated into the 456–466, 517–530, and 667–687 nm regions, respectively. **(e)** Tip-enhanced *2PPL* spatially integrated spectrum of the region at 667–687 nm. **Panel a,b,c,d**: Copyright 2021, ACS. Adapted with permission.[141]

© 2024 The Authors. ChemNanoMat published by Wiley-VCH GmbH

2199692x, 2024, 4, Downloaded from https://acces.onlinelibrary.wiley.com/doi/10.1002/cnma.202300566 by Universidad De Cantabria, Wiley Online Library on [07/08/2024]. See the Terms and Conditions (https://onlinelibrary.wiley.com/terms-and-conditions) on Wiley Online Library for rules of use; OA articles are governed by the applicable Creative Commons License

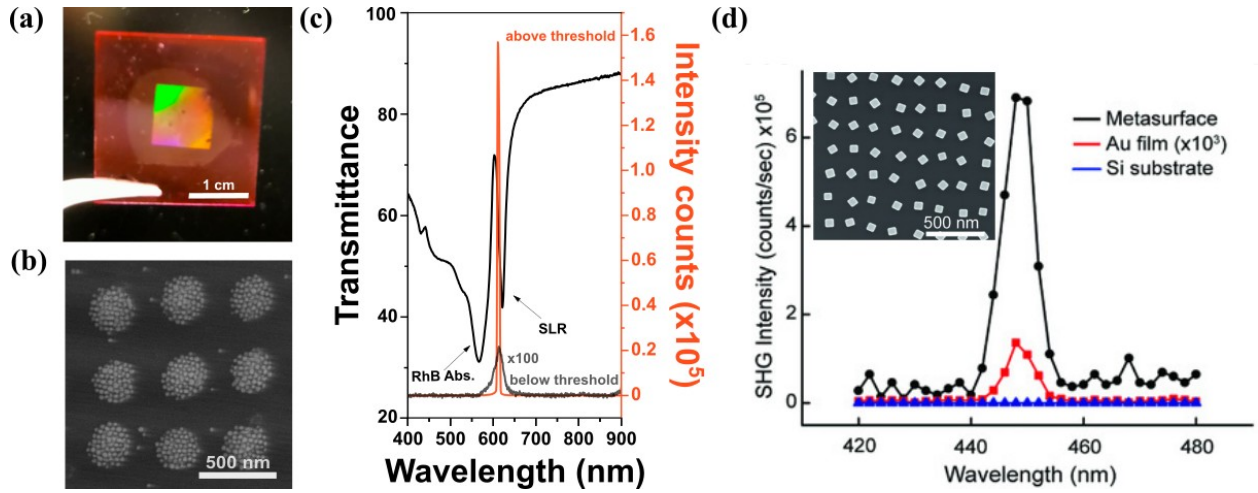

Figure 6. Colloidal-based plasmonic metasurfaces for non-linear optics. **(a)** photograph and **(b)** *SEM* image of a template-assisted self-assembled silver nanoparticle array on top of a layer of SU8 epoxy resin hosting the gain medium (Rhodamine B). **(c)** Lasing emission achieved by pumping the system using a 532 nm pulsed laser. **(d)** Silver nanocube-on-metal assembly for *SHG*. **Panel a,b,c**: Copyright 2023, Wiley-VCH. Adapted with permission.[115] **Panel d**: Copyright 2018, Wiley-VCH. Adapted with permission.[146]

5.2. Colloidal Systems for Non-Linear Optical Spectroscopies

Arguably, the field of chemistry where colloidal nanoparticles and metasurface applications hold the highest potential is most likely the one of molecular spectroscopies. Here, one can take full advantage of the rich surface chemistry of this type of system, encompassing small molecules, polymer shells, DNA, and antibodies. Like linear susceptivity, which contains information about the polarizability of the molecules, NLOS also provides rich chemical information, and depending on the molecular properties of interest, specific molecular transitions must be considered when designing spectroscopic experiments. The most common second- and third-order NLOS (Figure 1c) are SHG spectroscopy, vibrational sum frequency generation spectroscopy (vSFG), hyper Raman spectroscopy (HRS), femtosecond stimulated Raman spectroscopy (FSRS), and coherent anti-Stokes Raman spectroscopy (CARS).[147] For all of them, the plasmonic-enhanced version was demonstrated using colloidal nanoparticles. For example, SE-HRS found applications in diverse fields, including accessing single-photon forbidden excited states,[148] and two-photon vibrational microscopy[149] for biological tissues (Figure 7a);[150] Schlücker *et al.* used antibody-labeled gold/silver nanoshells to enhance the immune-contrast in surface-enhanced CARS (SE-CARS) microscopy[151] (Figure 7b); and Pluchery and coworkers used SE-vSFG to interrogate the capping ligands of gold nanoparticles.[152] However, the vSFG enhancement factors were reported to be only 21× for the signal from gold nanoparticles compared to Au(111) surfaces. Nonetheless, the higher signal enhancement could be achieved if the plasmonic metasurface would resonate with all the optical transition involved ($\omega_{IR,}$ $\omega_{vis,}$ and ω_{SFG}).

In addition to signal enhancement, the time-resolved capability of SE-CARS was demonstrated in 2012 by Scully and coworkers.[153] This study reported a molecular analyte's (pyridine-water complex) vibrational dephasing times greater than ten picoseconds for pyridine near nanoparticles. Around the same time, the groups of Frontiera and Van Duyne also reported the first demonstration of surface-enhanced FSRS (SE-FSRS)[154,155] (Figure 1c), where the femtosecond timescale gives access to several fundamental processes involving plasmonic resonances and molecular optical transitions (Figure 7c), such as phase-matching near metal surfaces,[156] and molecular vibrational dephasing.[157] These experimental and theoretical advances indicate the power of SE-NLOS not only in the signal enhancements but also for the study of the plasmon-molecule dynamics at the suitable timescale, which could play a major role in plasmon-mediated and strong-coupled chemistry. Overall, SE-NLOS mainly focused on the localized surface plasmon resonance of colloidal nanoparticles. Opportunities for using other plasmonic resonance systems, such as lattice resonances over large probe areas, remain unexplored.

6. Conclusions and Perspectives

We anticipate that the exploration of a "chemistry of metamaterials" will provide a renewed motivation in the use of colloidal plasmonic metasurfaces in the context of NL optical phenomena. Colloidal self-assembly has recently achieved the fabrication of optical cavities with quality factors that open new avenues for the interrogation of both NL absorption and emission processes, as well as NL molecular spectroscopies. In particular, by modifying the individual nanoparticle building blocks, the internal architecture of the repeating unit, and the overall geometry of the metasurface, it will be possible to engineer both localized and collective responses. NLOS involve optical excitations and scattering/emissions at multiple wavelengths that might be far apart. Due to the intricate challenges in the fabrication of suitable substrates for SE-NLOS techniques, that aim to enhance the performance of light scattering processes, the use of lattice resonance can make more feasible the process enhancement, either for the excitation or the NL

© 2024 The Authors. ChemNanoMat published by Wiley-VCH GmbH

2199692x, 2024, 4, Downloaded from https://aces.onlinelibrary.wiley.com/doi/10.1002/cnma.202300566 by Universidad De Cantabria, Wiley Online Library on [07/08/2024]. See the Terms and Conditions (https://onlinelibrary.wiley.com/terms-and-conditions) on Wiley Online Library for rules of use; OA articles are governed by the applicable Creative Commons License

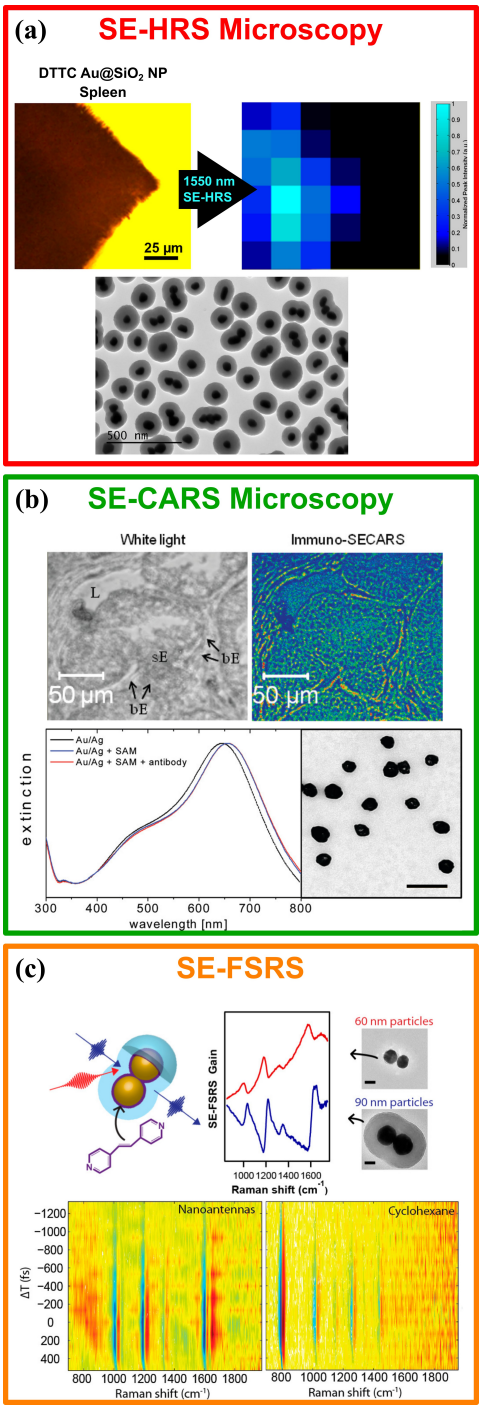

Figure 7. Colloidal non-linear optical spectroscopy and microscopy. **(a)** Bright-field image of the 3,3'-diethyl-thiatricarbocyanine iodide (*DTTC*) Au@SiO_2 nanoparticle spleen sample placed on a glass slide **(left)** and corresponding hyperspectral images of the 1550 nm *SE-HRS* **(right)**. On the bottom, transmission electron microscopy (*TEM*) image of the DTTC Au@SiO_2 nanoparticles displaying monomers and oligomers. **(b)** Immunochemistry based on *SE-CARS* for contrast generation. White light **(upper left)** and *SE-CARS* **(upper right)** images of prostate biopsies incubated with *SERS*-labeled p63 antibody. Extinction spectra **(left)** and *TEM* image **(right)** with scale bar 200 nm of bare gold/silver nanoshells. **(c)** Surface enhanced-femtosecond stimulated Raman spectroscopy (*SE-FSRS*) using nanoantennas made with Au@SiO2 core-shell nanoparticles encapsulating the Raman probe molecules. The plots on the bottom show the time-delay between pump and probes dependence of *SE-FSRS* data for nanoantennas samples **(left)** and the neat cyclohexane standard **(right)**. **Panel a**: Copyright 2022, Wiley-VCH. Adapted with permission.[149] **Panel b**: Copyright 2022, ACS. Adapted with permission.[151] **Panel c**: Copyright 2022, ACS. Adapted with permission.[55]

signal. Exploiting the flexibility offered by colloidal assembled nanoparticles array, it may be possible to engineer a metasurface that matches all the optical fields and uses the plasmon lifetime to tune into the desired process. The outcome of this research will enhance our comprehension of plasmonic near-fields and hold great promise for groundbreaking applications in various scientific and technological domains. Moreover, the surface chemistry and crystallographic control offered by the colloidal system could dramatically impact the application of this new generation of metamaterials for catalysis, sensing, and telecommunication.

List of Abbreviation

2PA	Two-photon Absorption.
2PPL	Two-photon Luminescence.
CAPA	Capillary-Assisted Particle Assembly.
CARS	Coherent Anti-Stokes Raman Scattering.
DFG	Difference Frequency Generation.
FSRS	Femtosecond Stimulated Raman Scattering.
FWM	Four Wave Mixing.
HRS	Hyper Raman Scattering.
IR	Infrared.
NIR	Near Infrared.
NL	Non-Linear.
SE-CARS	Surface-Enhanced Coherent Anti-Stokes Raman Scattering.
SE-FSRS	Surface-Enhanced Femtosecond Stimulated Raman Scattering.
SE-HRS	Surface-Enhanced Hyper Raman Spectroscopy.
SEM	Scanning Electron Microscopy.
SE-NLOS	Surface-Enhanced Non-Linear Optical Spectroscopy.
SERS	Surface-Enhanced Raman Spectroscopy.
SE-vSFG	Surface-Enhanced Vibrational Sum Frequency Generation Spectroscopy.
SFG	Sum Frequency Generation.
SHG	Second Harmonic Generation.
TASA	Template-Assisted Self-Assembly.
TEM	Transmission Electronic Microscopy.
THG	Third Harmonic Generation.
UV	Ultraviolet.
WS-SERES	Wavelength-Scanned Surface-Enhanced Raman Excitation Spectroscopy.

Acknowledgements

This project received funding from the Spanish Ministerio de Ciencia e Innovación through the grant FUNFUTURE (CEX2019-000917-S), in the framework of the Spanish Severo Ochoa Centre of Excellence program. L.S. and Y.C.'s research is supported by the 2020 Post-doctoral Junior Leader-Incoming Fellowship by "La Caixa" Foundation (ID 100010434, fellowship code LCF/BQ/PI20/11760028), and a 2022 Leonardo Grant for Researchers and Cultural Creators, BBVA Foundation. Y.C. acknowledges the auspices of the UAB material science doctoral

© 2024 The Authors. ChemNanoMat published by Wiley-VCH GmbH

2199692x, 2024, 4, Downloaded from https://aces.onlinelibrary.wiley.com/doi/10.1002/cnma.202300566 by Universidad De Cantabria, Wiley Online Library on [07/08/2024]. See the Terms and Conditions (https://onlinelibrary.wiley.com/terms-and-conditions) on Wiley Online Library for rules of use; OA articles are governed by the applicable Creative Commons License

program. N.C. acknowledges support from the US National Science Foundation (CHE-2304955).

Conflict of Interests

The authors declare no conflict of interest.

Data Availability Statement

Data sharing is not applicable to this article as no new data were created or analyzed in this study.

Keywords: plasmonic metasurfaces · colloidal self-assembly · nonlinear optics · nonlinear spectroscopy

[1] E. Hao, G. C. Schatz, *J. Chem. Phys.* **2003**, *120 (1)*, 357–366, https://doi.org/10.1063/1.1629280.
[2] S. Marhaba, G. Bachelier, C. Bonnet, M. Broyer, E. Cottancin, N. Grillet, J. Lermé, J.-L. Vialle, M. Pellarin, *J. Phys. Chem. C* **2009**, *113 (11)*, 4349–4356, https://doi.org/10.1021/jp810405y.
[3] N. J. Halas, S. Lal, W.-S. Chang, S. Link, P. Nordlander, *Chem. Rev.* **2011**, *111* (6), 3913–3961, https://doi.org/10.1021/cr200061k.
[4] E. Yablonovitch, *J. Opt. Soc. Am. B* **1993**, *10 (2)*, 283–295, https://doi.org/10.1364/JOSAB.10.000283.
[5] V. G. Veselago, *Sov. Phys. Usp.* **1968**, *10 (4)*, 509, https://doi.org/10.1070/PU1968v010n04ABEH003699.
[6] J. B. Pendry, *Phys. Rev. Lett.* **2000**, *85 (18)*, 3966–3969, https://doi.org/10.1103/PhysRevLett.85.3966.
[7] R. A. Shelby, D. R. Smith, S. Schultz, *Science* **2001**, *292 (5514)*, 77–79, https://doi.org/10.1126/science.1058847.
[8] D. Lin, P. Fan, E. Hasman, M. L. Brongersma, *Science* **2014**, *345 (6194)*, 298–302, https://doi.org/10.1126/science.1253213.
[9] N. Yu, P. Genevet, M. A. Kats, F. Aieta, J.-P. Tetienne, F. Capasso, Z. Gaburro, *Science* **2011**, *334 (6054)*, 333–337, https://doi.org/10.1126/science.1210713.
[10] S. Nie, I. F. Akyildiz, *Nat. Electron.* **2021**, *4 (3)*, 177–178, https://doi.org/10.1038/s41928-021-00555-3.
[11] Z. Li, X. Tian, C.-W. Qiu, J. S. Ho, *Nat. Electron.* **2021**, *4 (6)*, 382–391, https://doi.org/10.1038/s41928-021-00589-7.
[12] S. Abdollahramezani, O. Hemmatyar, M. Taghinejad, H. Taghinejad, A. Krasnok, A. A. Eftekhar, C. Teichrib, S. Deshmukh, M. A. El-Sayed, E. Pop, M. Wuttig, A. Alù, W. Cai, A. Adibi, *Nat. Commun.* **2022**, *13 (1)*, 1696, https://doi.org/10.1038/s41467-022-29374-6.
[13] X. Feng, X. Xie, M. Pu, X. Ma, Y. Guo, X. Li, X. Luo, *Opt. Express* **2020**, *28 (7)*, 9445–9453, https://doi.org/10.1364/OE.388335.
[14] M. Jang, Y. Horie, A. Shibukawa, J. Brake, Y. Liu, S. M. Kamali, A. Arbabi, H. Ruan, A. Faraon, C. Yang, *Nature Photon* **2018**, *12 (2)*, 84–90, https://doi.org/10.1038/s41566-017-0078-z.
[15] K. Aydin, V. E. Ferry, R. M. Briggs, H. A. Atwater, *Nat. Commun.* **2011**, *2 (1)*, 517, https://doi.org/10.1038/ncomms1528.
[16] I. Alves Oliveira, I. L. Gomes de Souza, V. F. Rodriguez-Esquerre, *Sci. Rep.* **2021**, *11 (1)*, 21919, https://doi.org/10.1038/s41598-021-01479-w.
[17] Y. G. Chen, T. S. Kao, B. Ng, X. Li, X. G. Luo, B. Luk'yanchuk, S. A. Maier, M. H. Hong, *Opt. Express* **2013**, *21 (11)*, 13691–13698, https://doi.org/10.1364/OE.21.013691.
[18] B. I. Karawdeniya, A. M. Damry, K. Murugappan, S. Manjunath, Y. M. N. D. Y. Bandara, C. J. Jackson, A. Tricoli, D. Neshev, *Chem. Rev.* **2022**, *122 (19)*, 14990–15030, https://doi.org/10.1021/acs.chemrev.1c00990.
[19] E. Cortés, F. J. Wendisch, L. Sortino, A. Mancini, S. Ezendam, S. Saris, L. de Menezes, A. Tittl, H. Ren, S. A. Maier, *Chem. Rev.* **2022**, *122(19)*, 15082–15176, https://doi.org/10.1021/acs.chemrev.2c00078.
[20] H. Lin, Z. Zhang, H. Zhang, K.-T. Lin, X. Wen, Y. Liang, Y. Fu, A. K. T. Lau, T. Ma, C.-W. Qiu, B. Jia, *Chem. Rev.* **2022**, *122 (19)*, 15204–15355, https://doi.org/10.1021/acs.chemrev.2c00048.
[21] P. Wang, A. V. Krasavin, L. Liu, Y. Jiang, Z. Li, X. Guo, L. Tong, A. V. Zayats, *Chem. Rev.* **2022**, *122 (19)*, 15031–15081, https://doi.org/10.1021/acs.chemrev.2c00333.
[22] R. W. Boyd, *Nonlinear Optics* – 4th Edition, Elsevier Inc, **2020**, pp 1–609, https://doi.org/10.1016/C2015-0-05510-1.
[23] A. Krasnok, M. Tymchenko, A. Alù, *Mater. Today* **2018**, *21 (1)*, 8–21, https://doi.org/10.1016/j.mattod.2017.06.007.
[24] I. Russier-Antoine, E. Benichou, G. Bachelier, C. Jonin, P. F. Brevet, *J. Phys. Chem. C* **2007**, *111 (26)*, 9044–9048, https://doi.org/10.1021/jp0675025.
[25] G. Bachelier, I. Russier-Antoine, E. Benichou, C. Jonin, P.-F. Brevet, *J. Opt. Soc. Am. B* **2008**, *25 (6)*, 955–960, https://doi.org/10.1364/JOSAB.25.000955.
[26] N. C. Panoiu, W. E. I. Sha, D. Y. Lei, G.-C. Li, *J. Opt.* **2018**, *20 (8)*, 083001, https://doi.org/10.1088/2040-8986/aac8ed.
[27] J. Butet, J. Duboisset, G. Bachelier, I. Russier-Antoine, E. Benichou, C. Jonin, P.-F. Brevet, *Nano Lett.* **2010**, *10 (5)*, 1717–1721, https://doi.org/10.1021/nl1000949.
[28] A. Capretti, G. F. Walsh, S. Minissale, J. Trevino, C. Forestiere, G. Miano, L. D. Negro, *Opt. Express* **2012**, *20 (14)*, 15797–15806, https://doi.org/10.1364/OE.20.015797.
[29] J. Nappa, G. Revillod, I. Russier-Antoine, E. Benichou, C. Jonin, P. F. Brevet, *Phys. Rev. B* **2005**, *71 (16)*, 165407, https://doi.org/10.1103/PhysRevB.71.165407.
[30] N. Segal, S. Keren-Zur, N. Hendler, T. Ellenbogen, *Nature Photon* **2015**, *9 (3)*, 180–184, https://doi.org/10.1038/nphoton.2015.17.
[31] D. L. Jeanmaire, R. P. Van Duyne, *J. Electroanal. Chem. Interfacial Electrochem.* **1977**, *84 (1)*, 1–20, https://doi.org/10.1016/S0022-0728(77)80224–6.
[32] M. G. Albrecht, J. A. Creighton, *J. Am. Chem. Soc.* **1977**, *99 (15)*, 5215–5217, https://doi.org/10.1021/ja00457a071.
[33] S. M. Morton, L. Jensen, *J. Am. Chem. Soc.* **2009**, *131 (11)*, 4090–4098, https://doi.org/10.1021/ja809143c.
[34] S. Nie, S. R. Emory, *Science* **1997**, *275 (5303)*, 1102–1106, https://doi.org/10.1126/science.275.5303.1102.
[35] R. Czaplicki, H. Husu, R. Siikanen, J. Mäkitalo, M. Kauranen, J. Laukkanen, J. Lehtolahti, M. Kuittinen, *Phys. Rev. Lett.* **2013**, *110 (9)*, 093902, https://doi.org/10.1103/PhysRevLett.110.093902.
[36] T. V. Konstantinova, P. N. Melent'ev, A. E. Afanas'ev, A. A. Kuzin, P. A. Starikov, A. S. Baturin, A. V. Tausenev, A. V. Konyashchenko, V. I. Balykin, *J. Exp. Theor. Phys.* **2013**, *117 (1)*, 21–31, https://doi.org/10.1134/S1063776113080165.
[37] K. Konishi, T. Higuchi, J. Li, J. Larsson, S. Ishii, M. Kuwata-Gonokami, *Phys. Rev. Lett.* **2014**, *112 (13)*, 135502, https://doi.org/10.1103/PhysRevLett.112.135502.
[38] W. Guo, B. Liu, Y. He, E. You, Y. Zhang, S. Huang, J. Wang, Z. Wang, *Nanomaterials* **2020**, *10 (12)*, 2557, https://doi.org/10.3390/nano10122557.
[39] Y. Pu, R. Grange, C.-L. Hsieh, D. Psaltis, *Phys. Rev. Lett.* **2010**, *104 (20)*, 207402, https://doi.org/10.1103/PhysRevLett.104.207402.
[40] J. Butet, G. Bachelier, I. Russier-Antoine, C. Jonin, E. Benichou, P.-F. Brevet, *Phys. Rev. Lett.* **2010**, *105 (7)*, 077401, https://doi.org/10.1103/PhysRevLett.105.077401.
[41] M. D. McMahon, D. Ferrara, C. T. Bowie, R. Lopez, R. F. Haglund Jr, *Appl. Phys. B* **2007**, *87 (2)*, 259–265, https://doi.org/10.1007/s00340-006-2569-3.
[42] D. Lis, Y. Caudano, M. Henry, S. Demoustier-Champagne, E. Ferain, F. Cecchet, *Adv. Opt. Mater.* **2013**, *1 (3)*, 244–255, https://doi.org/10.1002/adom.201200034.
[43] L. Carletti, D. Rocco, A. Locatelli, C. D. Angelis, V. F. Gili, M. Ravaro, I. Favero, G. Leo, M. Finazzi, L. Ghirardini, M. Celebrano, G. Marino, A. V. Zayats, *Nanotechnology* **2017**, *28 (11)*, 114005, https://doi.org/10.1088/1361-6528/aa5645.
[44] M. J. Huttunen, G. Bautista, M. Decker, S. Linden, M. Wegener, M. Kauranen, *Opt. Mater. Express* **2011**, *1 (1)*, 46–56, https://doi.org/10.1364/OME.1.000046.
[45] D. Kim, J. Yu, I. Hwang, S. Park, F. Demmerle, G. Boehm, M.-C. Amann, M. A. Belkin, J. Lee, *Nano Lett.* **2020**, *20 (11)*, 8032–8039, https://doi.org/10.1021/acs.nanolett.0c02978.
[46] G. Li, S. Chen, N. Pholchai, B. Reineke, P. W. H. Wong, E. Y. B. Pun, K. W. Cheah, T. Zentgraf, S. Zhang, *Nat. Mater.* **2015**, *14 (6)*, 607–612, https://doi.org/10.1038/nmat4267.
[47] F. Spreyer, J. Mun, H. Kim, R. M. Kim, K. T. Nam, J. Rho, T. Zentgraf, *ACS Photonics* **2022**, *9 (3)*, 784–792, https://doi.org/10.1021/acsphotonics.1c00882.

© 2024 The Authors. ChemNanoMat published by Wiley-VCH GmbH

2199692x, 2024, 4, Downloaded from https://acses.onlinelibrary.wiley.com/doi/10.1002/cnma.202300566 by Universidad De Cantabria, Wiley Online Library on [07/08/2024]. See the Terms and Conditions (https://onlinelibrary.wiley.com/terms-and-conditions) on Wiley Online Library for rules of use; OA articles are governed by the applicable Creative Commons License

[48] Y. Liu, L. Ma, S. Jiang, C. Han, P. Tang, H. Yang, X. Duan, N. Liu, H. Yan, X. Lan, *ACS Nano* **2021**, *15 (10)*, 16664–16672, https://doi.org/10.1021/acsnano.1c06639.
[49] J. Berthelot, G. Bachelier, M. Song, P. Rai, G. C. des Francs, A. Dereux, A. Bouhelier, *Opt. Express* **2012**, *20 (10)*, 10498–10508, https://doi.org/10.1364/OE.20.010498.
[50] K. D. Ko, A. Kumar, K. H. Fung, R. Ambekar, G. L. Liu, N. X. Fang, K. C. Toussaint Jr., *Nano Lett.* **2011**, *11 (1)*, 61–65, https://doi.org/10.1021/nl102751 m.
[51] A. Noor, A. R. Damodaran, I.-H. Lee, S. A. Maier, S.-H. Oh, C. Ciracì, *ACS Photonics* **2020**, *7 (12)*, 3333–3340, https://doi.org/10.1021/acsphotonics.0c01545.
[52] B. Metzger, T. Schumacher, M. Hentschel, M. Lippitz, H. Giessen, *ACS Photonics* **2014**, *1 (6)*, 471–476, https://doi.org/10.1021/ph5000677.
[53] R. Czaplicki, A. Kiviniemi, J. Laukkanen, J. Lehtolahti, M. Kuittinen, M. Kauranen, *Opt. Lett.* **2016**, *41 (12)*, 2684–2687, https://doi.org/10.1364/OL.41.002684.
[54] K. D. Ko, A. Kumar, K. H. Fung, R. Ambekar, G. L. Liu, N. X. Fang, K. C. Toussaint Jr. *Nano Lett.* **2011**, *11 (1)*, 61–65, https://doi.org/10.1021/nl102751 m.
[55] R. Czaplicki, A. Kiviniemi, M. J. Huttunen, X. Zang, T. Stolt, I. Vartiainen, J. Butet, M. Kuittinen, O. J. F. Martin, M. Kauranen, *Nano Lett.* **2018**, *18 (12)*, 7709–7714, https://doi.org/10.1021/acs.nanolett.8b03378.
[56] G. Li, S. Zhang, T. Zentgraf, *Nat. Rev. Mater.* **2017**, *2 (5)*, 1–14, https://doi.org/10.1038/natrevmats.2017.10.
[57] J. Butet, P.-F. Brevet, O. J. F. Martin, *ACS Nano* **2015**, *9 (11)*, 10545–10562, https://doi.org/10.1021/acsnano.5b04373.
[58] N. Accanto, J. B. Nieder, L. Piatkowski, M. Castro-Lopez, F. Pastorelli, D. Brinks, N. F. van Hulst, *Light-Sci. Appl.* **2014**, *3 (1)*, e143–e143, https://doi.org/10.1038/lsa.2014.24.
[59] N. I. Zheludev, V. I. Emel Yanov, *J. Opt. A: Pure Appl. Opt.* **2004**, *6 (1)*, 26–28, https://doi.org/10.1088/1464-4258/6/1/006.
[60] R. Kolkowski, J. Szeszko, B. Dwir, E. Kapon, J. Zyss, *Laser Photonics Rev.* **2016**, *10 (2)*, 287–298, https://doi.org/10.1002/lpor.201500212.
[61] G. F. Walsh, L. Dal Negro, *Nano Lett.* **2013**, *13 (7)*, 3111–3117, https://doi.org/10.1021/nl401037n.
[62] T. Abir, M. Tal, T. Ellenbogen, *Nano Lett.* **2022**, *22 (7)*, 2712–2717, https://doi.org/10.1021/acs.nanolett.1c04584.
[63] E. Almeida, O. Bitton, Y. Prior, *Nat. Commun.* **2016**, *7 (1)*, 12533, https://doi.org/10.1038/ncomms12533.
[64] S. Linden, F. B. P. Niesler, J. Förstner, Y. Grynko, T. Meier, M. Wegener, *Phys. Rev. Lett.* **2012**, *109 (1)*, 015502, https://doi.org/10.1103/PhysRevLett.109.015502.
[65] V. K. Valev, J. J. Baumberg, B. De Clercq, N. Braz, X. Zheng, E. J. Osley, S. Vandendriessche, M. Hojeij, C. Blejean, J. Mertens, C. G. Biris, V. Volskiy, M. Ameloot, Y. Ekinci, G. a. E. Vandenbosch, P. A. Warburton, V. V. Moshchalkov, N. C. Panoiu, *Adv. Mater.* **2014**, *26 (24)*, 4074–4081, https://doi.org/10.1002/adma.201401021.
[66] R. Czaplicki, A. Kiviniemi, M. J. Huttunen, X. Zang, T. Stolt, I. Vartiainen, J. Butet, M. Kuittinen, O. J. F. Martin, M. Kauranen, *Nano Lett.* **2018**, *18 (12)*, 7709–7714, https://doi.org/10.1021/acs.nanolett.8b03378.
[67] M. Celebrano, X. Wu, M. Baselli, S. Großmann, P. Biagioni, A. Locatelli, C. De Angelis, G. Cerullo, R. Osellame, B. Hecht, L. Duò, F. Ciccacci, M. Finazzi, *Nat. Nanotechnol.* **2015**, *10 (5)*, 412–417, https://doi.org/10.1038/nnano.2015.69.
[68] S. S. Masango, R. A. Hackler, N. Large, A.-I. Henry, M. O. McAnally, G. C. Schatz, P. C. Stair, R. P. Van Duyne, *Nano Lett.* **2016**, *16 (7)*, 4251–4259. https://doi.org/10.1021/acs.nanolett.6b01276.
[69] S. M. Stranahan, E. J. Titus, K. A. Willets, *J. Phys. Chem. Lett.* **2011**, *2 (21)*, 2711–2715, https://doi.org/10.1021/jz201133p.
[70] X. Li, G. Haberfehlner, U. Hohenester, O. Stéphan, G. Kothleitner, M. Kociak, *Science* **2021**, *371 (6536)*, 1364–1367, https://doi.org/10.1126/science.abg0330.
[71] A. Polman, M. Kociak, F. J. García de Abajo, *Nat. Mater.* **2019**, *18 (11)*, 1158–1171, https://doi.org/10.1038/s41563-019-0409-1.
[72] A. Losquin, L. F. Zagonel, V. Myroshnychenko, B. Rodríguez-González, M. Tencé, L. Scarabelli, J. Förstner, L. M. Liz-Marzán, F. J. García de Abajo, O. Stéphan, M. Kociak, *Nano Lett.* **2015**, *15 (2)*, 1229–1237, https://doi.org/10.1021/nl5043775.
[73] A. Bhattarai, A. Krayev, A. Temiryazev, D. Evplov, K. T. Crampton, W. P. Hess, P. Z. El-Khoury, *Nano Lett.* **2018**, *18 (6)*, 4029–4033, https://doi.org/10.1021/acs.nanolett.8b01690.
[74] A. D. McFarland, M. A. Young, J. A. Dieringer, R. P. Van Duyne, *J. Phys. Chem. B* **2005**, *109 (22)*, 11279–11285, https://doi.org/10.1021/jp050508u.
[75] J. Zhao, J. A. Dieringer, X. Zhang, G. C. Schatz, R. P. Van Duyne, *J. Phys. Chem. C* **2008**, *112 (49)*, 19302–19310, https://doi.org/10.1021/jp807837 t.
[76] P. D. Jr. Simmons, H. K. Turley, D. W. Silverstein, L. Jensen, J. P. Camden, *J. Phys. Chem. Lett.* **2015**, *6 (24)*, 5067–5071, https://doi.org/10.1021/acs.jpclett.5b02342.
[77] J. T. Golab, J. R. Sprague, K. T. Carron, G. C. Schatz, R. P. Van Duyne, *J. Chem. Phys.* **1988**, *88 (12)*, 7942–7951, https://doi.org/10.1063/1.454251.
[78] S. Nie, L. A. Lipscomb, S. Feng, N.-T. Yu, *Chem. Phys. Lett.* **1990**, *167 (1)*, 35–40, https://doi.org/10.1016/0009-2614(90)85066-L.
[79] F. Madzharova, Z. Heiner, J. Kneipp, *Chem. Soc. Rev.* **2017**, *46 (13)*, 3980–3999, https://doi.org/10.1039/C7CS00137 A.
[80] J. C. Hulteen, M. A. Young, R. P. Van Duyne, *Langmuir* **2006**, *22 (25)*, 10354–10364, https://doi.org/10.1021/la0612264.
[81] S. Baldelli, A. S. Eppler, E. Anderson, Y.-R. Shen, G. A. Somorjai, *J. Chem. Phys.* **2000**, *113 (13)*, 5432–5438, https://doi.org/10.1063/1.1290024.
[82] L. A. Dick, A. D. McFarland, C. L. Haynes, R. P. Van Duyne, *J. Phys. Chem. B* **2002**, *106 (4)*, 853–860, https://doi.org/10.1021/jp013638l.
[83] W. Zhang, H. Yu, H. Wu, P. S. Halasyamani, *Chem. Mater.* **2017**, *29 (7)*, 2655–2668, https://doi.org/10.1021/acs.chemmater.7b00243.
[84] L. Le Xuan, C. Zhou, A. Slablab, D. Chauvat, C. Tard, S. Perruchas, T. Gacoin, P. Villeval, J.-F. Roch, *Small* **2008**, *4 (9)*, 1332–1336, https://doi.org/10.1002/smll.200701093.
[85] S. Y. Chou, P. R. Krauss, P. J. Renstrom, *Science* **1996**, *272 (5258)*, 85–87, https://doi.org/10.1126/science.272.5258.85.
[86] N. Chiang, L. Scarabelli, G. A. Vinnacombe-Willson, L. A. Pérez, C. Dore, A. Mihi, S. J. Jonas, P. S. Weiss, *ACS Materials Lett.* **2021**, *3 (3)*, 282–289, https://doi.org/10.1021/acsmaterialslett.0c00535.
[87] C. Yesildag, Z. Ouyang, Z. Zhang, M. C. Lensen, *Front. Chem.* **2019**, *6*, 667, https://doi.org/10.3389/fchem.2018.00667.
[88] J. Chen, P. Mela, M. Möller, M. C. Lensen, *ACS Nano* **2009**, *3 (6)*, 1451–1456, https://doi.org/10.1021/nn9002924.
[89] Y. Brasse, V. Gupta, H. C. T. Schollbach, M. Karg, T. A. F. König, A. Fery, *Adv. Mater. Interfaces* **2020**, *7 (5)*, 1901678, https://doi.org/10.1002/admi.201901678.
[90] V. Gupta, P. T. Probst, F. R. Goßler, A. M. Steiner, J. Schubert, Y. Brasse, T. A. F. König, A. Fery, *ACS Appl. Mater. Interfaces* **2019**, *11 (31)*, 28189–28196, https://doi.org/10.1021/acsami.9b08871.
[91] L. Scarabelli, D. Vila-Liarte, A. Mihi, L. M. Liz-Marzán, *Acc. Mater. Res.* **2021**, *2 (9)*, 816–827, https://doi.org/10.1021/accountsmr.1c00106.
[92] M. Mayer, M. J. Schnepf, T. A. F. König, A. Fery, *Adv. Opt. Mater.* **2019**, *7 (1)*, 1800564, https://doi.org/10.1002/adom.201800564.
[93] M. Karg, T. A. F. König, M. Retsch, C. Stelling, P. M. Reichstein, T. Honold, M. Thelakkat, A. Fery, *Mater. Today* **2015**, *18 (4)*, 185–205, https://doi.org/10.1016/j.mattod.2014.10.036.
[94] Z. Li, Q. Fan, Y. Yin, *Chem. Rev.* **2022**, *122 (5)*, 4976–5067, https://doi.org/10.1021/acs.chemrev.1c00482.
[95] N. Vogel, M. Retsch, C.-A. Fustin, A. del Campo, U. Jonas, *Chem. Rev.* **2015**, *115 (13)*, 6265–6311, https://doi.org/10.1021/cr400081d.
[96] G. A. Vinnacombe-Willson, J. K. Lee, N. Chiang, L. Scarabelli, S. Yue, R. Foley, I. Frost, P. S. Weiss, S. J. Jonas, *ACS Appl. Nano Mater.* **2023**, *6 (8)*, 6454–6460, https://doi.org/10.1021/acsanm.3c00440.
[97] G. A. Vinnacombe-Willson, Y. Conti, S. J. Jonas, P. S. Weiss, A. Mihi, L. Scarabelli, *Adv. Mater.* **2022**, *34 (37)*, 2205330, https://doi.org/10.1002/adma.202205330.
[98] L. Liz-Marzán, *Colloidal Synthesis of Plasmonic Nanometals*, CRC Press, The Copyright Jenny Stanford Publishing Pte.Ltd, **2020**, pp 1–867.
[99] L. Scarabelli, M. Sun, X. Zhuo, S. Yoo, J. E. Millstone, M. R. Jones, L. M. Liz-Marzán, *Chem. Rev.* **2023**, *123 (7)*, 3493–3542, https://doi.org/10.1021/acs.chemrev.3c00033.
[100] J. Karst, M. Hentschel, N. H. Cho, H. Kim, K. T. Nam, H. Giessen, *Plasmonic Materials and Metastructures*; S. Gwo, A. Alù, X. Li, C.-K. Shih, Eds.; Materials Today; Elsevier, **2024**; pp 285–317, https://doi.org/10.1016/B978-0-323-85379-8.00010–1.
[101] T. B. Hoang, G. M. Akselrod, C. Argyropoulos, J. Huang, D. R. Smith, M. H. Mikkelsen, *Nat. Commun.* **2015**, *6 (1)*, 7788, https://doi.org/10.1038/ncomms8788.
[102] Y. Brasse, M. B. Müller, M. Karg, C. Kuttner, T. A. F. König, A. Fery, *ACS Appl. Mater. Interfaces* **2018**, *10 (3)*, 3133–3141, https://doi.org/10.1021/acsami.7b16941.
[103] J. Chen, P. Dong, D. Di, C. Wang, H. Wang, J. Wang, X. Wu, *Appl. Surf. Sci.* **2013**, *270*, 6–15, https://doi.org/10.1016/j.apsusc.2012.11.165.
[104] K. Volk, J. P. S. Fitzgerald, M. Retsch, M. Karg, *Adv. Mater.* **2015**, *27 (45)*, 7332–7337, https://doi.org/10.1002/adma.201503672.

© 2024 The Authors. ChemNanoMat published by Wiley-VCH GmbH

2199692x, 2024, 4, Downloaded from https://acses.onlinelibrary.wiley.com/doi/10.1002/cnma.202300566 by Universidad De Cantabria, Wiley Online Library on [07/08/2024]. See the Terms and Conditions (https://onlinelibrary.wiley.com/terms-and-conditions) on Wiley Online Library for rules of use; OA articles are governed by the applicable Creative Commons License

[105] P. Chattopadhyay, L. Wang, A. Eychmüller, J. Simmchen, *J. Chem. Educ.* **2022**, *99 (2)*, 952–956, https://doi.org/10.1021/acs.jchemed.1c00667.
[106] S. Ni, H. Wolf, L. Isa, *Langmuir* **2018**, *34 (7)*, 2481–2488, https://doi.org/10.1021/acs.langmuir.7b03944.
[107] M. Rycenga, P. H. C. Camargo, Y. Xia, *Soft Matter* **2009**, *5 (6)*, 1129–1136, https://doi.org/10.1039/B811021B.
[108] H. Agrawal, E. C. Garnett, *ACS Nano* **2020**, *14 (9)*, 11009–11016, https://doi.org/10.1021/acsnano.0c04793.
[109] M. Juodėnas, T. Tamulevičius, J. Henzie, D. Erts, S. Tamulevičius, *ACS Nano* **2019**, *13 (8)*, 9038–9047, https://doi.org/10.1021/acsnano.9b03191.
[110] V. Flauraud, M. Mastrangeli, G. D. Bernasconi, J. Butet, D. T. L. Alexander, E. Shahrabi, O. J. F. Martin, J. Brugger, *Nat. Nanotechnol.* **2017**, *12 (1)*, 73–80, https://doi.org/10.1038/nnano.2016.179.
[111] M. Juodėnas, D. Peckus, T. Tamulevičius, Y. Yamauchi, S. Tamulevičius, J. Henzie, *ACS Photonics* **2020**, *7 (11)*, 3130–3140, https://doi.org/10.1021/acsphotonics.0c01187.
[112] C. Hanske, M. Tebbe, C. Kuttner, V. Bieber, V. V. Tsukruk, M. Chanana, T. A. F. König, A. Fery, *Nano Lett.* **2014**, *14 (12)*, 6863–6871, https://doi.org/10.1021/nl502776s.
[113] A. Rey, G. Billardon, E. Lörtscher, K. Moth-Poulsen, N. Stuhr-Hansen, H. Wolf, T. Bjørnholm, A. Stemmer, H. Riel, *Nanoscale* **2013**, *5 (18)*, 8680–8688, https://doi.org/10.1039/C3NR02358C.
[114] J. B. Lee, H. Walker, Y. Li, T. W. Nam, A. Rakovich, R. Sapienza, Y. S. Jung, Y. S. Nam, S. A. Maier, E. Cortés, *ACS Nano* **2020**, *14 (12)*, 17693–17703, https://doi.org/10.1021/acsnano.0c09319.
[115] Y. Conti, N. Passarelli, J. Mendoza-Carreño, L. Scarabelli, A. Mihi, *Adv. Opt. Mater.* **2023**, *11 (23)*, 2300983. https://doi.org/10.1002/adom.202300983.
[116] M. Mayer, M. Tebbe, C. Kuttner, M. J. Schnepf, T. A. F. König, A. Fery, *Faraday Discuss.* **2016**, *191 (0)*, 159–176, https://doi.org/10.1039/C6FD00013D.
[117] K. Volk, J. P. S. Fitzgerald, P. Ruckdeschel, M. Retsch, T. A. F. König, M. Karg, *Adv. Opt. Mater.* **2017**, *5 (9)*, 1600971, https://doi.org/10.1002/adom.201600971.
[118] M. A. Fernández-Rodríguez, R. Elnathan, R. Ditcovski, F. Grillo, G. M. Conley, F. Timpu, A. Rauh, K. Geisel, T. Ellenbogen, R. Grange, F. Scheffold, M. Karg, W. Richtering, N. H. Voelcker, L. Isa, *Nanoscale* **2018**, *10 (47)*, 22189–22195, https://doi.org/10.1039/C8NR07059H.
[119] G. A. Vinnacombe-Willson, Y. Conti, A. Stefancu, P. S. Weiss, E. Cortés, L. Scarabelli, *Chem. Rev.* **2023**, *123 (13)*, 8488–8529, https://doi.org/10.1021/acs.chemrev.2c00914.
[120] R. D. Neal, Z. R. Lawson, W. J. Tuff, K. Xu, V. Kumar, M. T. Korsa, M. Zhukovskyi, M. R. Rosenberger, J. Adam, J. A. Hachtel, J. P. Camden, R. A. Hughes, S. Neretina, *Small* **2022**, *18 (52)*, 2205780, https://doi.org/10.1002/smll.202205780.
[121] R. D. Neal, R. A. Hughes, A. S. Preston, S. D. Golze, T. B. Demille, S. Neretina, *J. Mater. Chem. C* **2021**, *9* (38), 12974–13012. https://doi.org/10.1039/D1TC01494C.
[122] G. A. Vinnacombe-Willson, Y. Conti, S. J. Jonas, P. S. Weiss, A. Mihi, L. Scarabelli, *Adv. Mater.* **2022**, *34(37)*, 2205330. https://doi.org/10.1002/adma.202205330.
[123] Q.-Y. Lin, J. A. Mason, Z. Li, W. Zhou, M. N. O'Brien, K. A. Brown, M. R. Jones, S. Butun, B. Lee, V. P. Dravid, K. Aydin, C. A. Mirkin, *Science* **2018**, *359 (6376)*, 669–672, https://doi.org/10.1126/science.aaq0591.
[124] J. A. Fan, K. Bao, L. Sun, J. Bao, V. N. Manoharan, P. Nordlander, F. Capasso, *Nano Lett.* **2012**, *12 (10)*, 5318–5324, https://doi.org/10.1021/nl302650t.
[125] C. Hanske, G. González-Rubio, C. Hamon, P. Formentín, E. Modin, A. Chuvilin, A. Guerrero-Martínez, L. F. Marsal, L. M. Liz-Marzán, *J. Phys. Chem. C* **2017**, *121 (20)*, 10899–10906, https://doi.org/10.1021/acs.jpcc.6b12161.
[126] D. A. Yashunin, A. I. Korytin, A. I. Smirnov, A. N. Stepanov, *J. Phys. D* **2016**, *49 (10)*, 105107, https://doi.org/10.1088/0022-3727/49/10/105107.
[127] C. Molinaro, Y. El Harfouch, E. Palleau, F. Eloi, S. Marguet, L. Douillard, F. Charra, C. Fiorini-Debuisschert, *J. Phys. Chem. C* **2016**, *120 (40)*, 23136–23143, https://doi.org/10.1021/acs.jpcc.6b07498.
[128] F. Han, Z. Guan, T. S. Tan, Q.-H. Xu, *ACS Appl. Mater. Interfaces* **2012**, *4 (9)*, 4746–4751, https://doi.org/10.1021/am301121k.
[129] C. Jiang, T. Zhao, P. Yuan, N. Gao, Y. Pan, Z. Guan, N. Zhou, Q.-H. Xu, *ACS Appl. Mater. Interfaces* **2013**, *5 (11)*, 4972–4977, https://doi.org/10.1021/am4007403.
[130] T. Zhao, X.-F. Jiang, N. Gao, S. Li, N. Zhou, R. Ma, Q.-H. Xu, *J. Phys. Chem. B* **2013**, *117 (49)*, 15576–15583, https://doi.org/10.1021/jp405929w.
[131] H.-D. Deng, G.-C. Li, Q.-F. Dai, M. Ouyang, S. Lan, V. A. Trofimov, T. M. Lysak, *Nanotechnology* **2013**, *24 (7)*, 075201, https://doi.org/10.1088/0957-4484/24/7/075201.
[132] G. T. Boyd, Z. H. Yu, Y. R. Shen, *Phys. Rev. B* **1986**, *33 (12)*, 7923–7936, https://doi.org/10.1103/PhysRevB.33.7923.
[133] K. Imura, H. Okamoto, *J. Phys. Chem. C* **2009**, *113* (27), 11756–11759, https://doi.org/10.1021/jp9018074.
[134] A. Bouhelier, R. Bachelot, G. Lerondel, S. Kostcheev, P. Royer, G. P. Wiederrecht, *Phys. Rev. Lett.* **2005**, *95 (26)*, 267405, https://doi.org/10.1103/PhysRevLett.95.267405.
[135] A. Gaiduk, M. Yorulmaz, M. Orrit, *ChemPhysChem* **2011**, *12 (8)*, 1536–1541, https://doi.org/10.1002/cphc.201100167.
[136] H. Zhu, M. Garai, Z. Chen, Q.-H. Xu, *J. Phys. Chem. C* **2017**, *121 (51)*, 28546–28555, https://doi.org/10.1021/acs.jpcc.7b10235.
[137] D. A. Yashunin, N. V. Ilin, A. N. Stepanov, A. I. Smirnov, *J. Phys. D* **2014**, *47 (30)*, 305102, https://doi.org/10.1088/0022-3727/47/30/305102.
[138] T. Jägeler-Hoheisel, J. Cordeiro, O. Lecarme, A. Cuche, C. Girard, E. Dujardin, D. Peyrade, A. Arbouet, *J. Phys. Chem. C* **2013**, *117 (44)*, 23126–23132, https://doi.org/10.1021/jp406410k.
[139] F. Helmchen, W. Denk, *Nat. Methods* **2005**, *2 (12)*, 932–940, https://doi.org/10.1038/nmeth818.
[140] J. Olesiak-Banska, M. Waszkielewicz, P. Obstarczyk, M. Samoc, *Chem. Soc. Rev.* **2019**, *48 (15)*, 4087–4117, https://doi.org/10.1039/C8CS00849C.
[141] C.-F. Wang, P. Z. El-Khoury, *J. Phys. Chem. Lett.* **2021**, *12 (44)*, 10761–10765, https://doi.org/10.1021/acs.jpclett.1c03196.
[142] V. Krivenkov, P. Samokhvalov, A. Sánchez-Iglesias, M. Grzelczak, I. Nabiev, Y. Rakovich, *Nanoscale* **2021**, *13 (8)*, 4614–4623, https://doi.org/10.1039/D0NR08893E.
[143] E. Dulkeith, T. Niedereichholz, T. Klar, J. Feldmann, G. Von Plessen, D. Gittins, K. Mayya, F. Caruso, *Phys. Rev. B* **2004**, *70 (20)*, 205424, https://doi.org/10.1103/PhysRevB.70.205424.
[144] V. G. Kravets, A. V. Kabashin, W. L. Barnes, A. N. Grigorenko, *Chem. Rev.* **2018**, *118 (12)*, 5912–5951, https://doi.org/10.1021/acs.chemrev.8b00243.
[145] X. Liu, X. Jia, M. Fischer, Z. Huang, D. R. Smith, *Nano Lett.* **2018**, *18 (10)*, 6181–6187, https://doi.org/10.1021/acs.nanolett.8b02042.
[146] Y. Zeng, H. Qian, M. J. Rozin, Z. Liu, A. R. Tao, *Adv. Funct. Mater.* **2018**, *28 (51)*, 1803019, https://doi.org/10.1002/adfm.201803019.
[147] N. L. Gruenke, M. F. Cardinal, M. O. McAnally, R. R. Frontiera, G. C. Schatz, R. P. V. Duyne, *Chem. Soc. Rev.* **2016**, *45 (8)*, 2263–2290, https://doi.org/10.1039/C5CS00763A.
[148] C. B. Milojevich, D. W. Silverstein, L. Jensen, J. P. Camden, *ChemPhysChem* **2011**, *12 (1)*, 101–103, https://doi.org/10.1002/cphc.201000868.
[149] J. E. Olson, J. H. Yu, R. L. Thimes, J. P. Camden, *J. Biophotonics* **2022**, *15 (1)*, e202100158, https://doi.org/10.1002/jbio.202100158.
[150] K. Turley, P. Camden, *Chem. Commun.* **2014**, *50 (12)*, 1472–1474, https://doi.org/10.1039/C3CC49002E.
[151] S. Schlücker, M. Salehi, G. Bergner, M. Schütz, P. Ströbel, A. Marx, I. Petersen, B. Dietzek, J. Popp, *Anal. Chem.* **2011**, *83 (18)*, 7081–7085, https://doi.org/10.1021/ac201284d.
[152] O. Pluchery, C. Humbert, M. Valamanesh, E. Lacaze, B. Busson, *Phys. Chem. Chem. Phys.* **2009**, *11 (35)*, 7729–7737, https://doi.org/10.1039/B902142F.
[153] D. V. Voronine, A. M. Sinyukov, X. Hua, K. Wang, P. K. Jha, E. Munusamy, S. E. Wheeler, G. Welch, A. V. Sokolov, M. O. Scully, *Sci. Rep.* **2012**, *2 (1)*, 891, https://doi.org/10.1038/srep00891.
[154] R. R. Frontiera, A.-I. Henry, N. L. Gruenke, R. P. Van Duyne, *J. Phys. Chem. Lett.* **2011**, *2 (10)*, 1199–1203, https://doi.org/10.1021/jz200498z.
[155] R. R. Frontiera, N. L. Gruenke, R. P. Van Duyne, *Nano Lett.* **2012**, *12 (11)*, 5989–5994, https://doi.org/10.1021/nl303488 m.
[156] J. A. Parkhill, D. Rappoport, A. Aspuru-Guzik, *J. Phys. Chem. Lett.* **2011**, *2 (15)*, 1849–1854, https://doi.org/10.1021/jz2005573.
[157] D. P. Hoffman, R. A. Mathies, *Acc. Chem. Res.* **2016**, *49 (4)*, 616–625, https://doi.org/10.1021/acs.accounts.5b00508.

Manuscript received: November 21, 2023
Revised manuscript received: January 29, 2024
Accepted manuscript online: February 19, 2024
Version of record online: March 8, 2024

© 2024 The Authors. ChemNanoMat published by Wiley-VCH GmbH

2199692x, 2024, 4, Downloaded from https://acces.onlinelibrary.wiley.com/doi/10.1002/cnma.202300566 by Universidad De Cantabria, Wiley Online Library on [07/08/2024]. See the Terms and Conditions (https://onlinelibrary.wiley.com/terms-and-conditions) on Wiley Online Library for rules of use; OA articles are governed by the applicable Creative Commons License